

Journal of Materials Chemistry A

Accepted Manuscript



This is an *Accepted Manuscript*, which has been through the Royal Society of Chemistry peer review process and has been accepted for publication.

Accepted Manuscripts are published online shortly after acceptance, before technical editing, formatting and proof reading. Using this free service, authors can make their results available to the community, in citable form, before we publish the edited article. We will replace this *Accepted Manuscript* with the edited and formatted *Advance Article* as soon as it is available.

You can find more information about *Accepted Manuscripts* in the [Information for Authors](#).

Please note that technical editing may introduce minor changes to the text and/or graphics, which may alter content. The journal's standard [Terms & Conditions](#) and the [Ethical guidelines](#) still apply. In no event shall the Royal Society of Chemistry be held responsible for any errors or omissions in this *Accepted Manuscript* or any consequences arising from the use of any information it contains.

Cite this: DOI: 10.1039/c0xx00000x

PAPER

www.rsc.org/xxxxxx

Enhanced open-circuit voltage in polymer solar cells by dithieno[3,2-*b*:2',3'-*d*]pyrrole N-acylation

Wouter Vanormelingen,^{a,b} Jurgen Kesters,^{a,b,c} Pieter Verstappen,^{a,b} Jeroen Drijkoningen,^{b,c} Julija Kudrjasova,^{a,b} Simplicie Koudjina,^d Vincent Liégeois,^d Benoît Champagne,^d Jean Manca,^{b,c} Laurence Lutsen,^b Dirk Vanderzande^{a,b} and Wouter Maes^{*a,b}

Received (in XXX, XXX) Xth XXXXXXXXXX 20XX, Accepted Xth XXXXXXXXXX 20XX

DOI: 10.1039/b000000x

A series of low bandgap copolymers composed of N-acyl-substituted dithieno[3,2-*b*:2',3'-*d*]pyrroles (DTP's) as the electron rich donor constituents (with various alkyl side chain patterns) combined with 10 different electron deficient acceptor building blocks are developed for polymer solar cell applications. Due to the introduction of the N-acyl substituents, the HOMO energy levels of the push-pull copolymers decrease as compared to the N-alkyl-DTP analogues, resulting in an increased open-circuit voltage (V_{oc}) and hence solar cell performance. For an N-acyl-DTP-*alt*-thieno[3,4-*c*]pyrrole-4,6-dione (PDTP-TPD) copolymer a bulk heterojunction device with a V_{oc} up to 0.80 V and a power conversion efficiency of 15 4.0% is obtained, the highest value for DTP-based polymer materials to date. Moreover, by implementation of a conjugated polyelectrolyte cathode interlayer the short-circuit current noticeably increases, enhancing the solar cell efficiency to 5.8%.

Introduction

Polymer solar cells (PSC's) are studied extensively since they 20 offer the potential of low-cost solution processing and manufacturing of large areas via (roll-to-roll) printing technologies.¹ Furthermore, they can be produced with tuneable colour and transparency on flexible substrates and they are light-weight, attractive features that allow to target photovoltaic (PV) 25 applications and products beyond traditional Si-based PV. Through careful molecular and device engineering the power conversion efficiencies (PCE's) of bulk heterojunction (BHJ) PSC's have steadily increased to over 9%.^{1,2} The photoactive layer of high performance BHJ PSC devices consists of an intimate blend of a low bandgap electron donor polymer and a 30 fullerene acceptor (most often [6,6]-phenyl-C₇₁-butyric acid methyl ester or PC₇₁BM). The state of the art low bandgap copolymers are composed of alternating electron rich (donor) and electron poor (acceptor) heterocyclic moieties, affording 35 intramolecular charge transfer and thereby broadening the absorption window. Conjugated polymer engineering mostly focuses on the design and variation of the donor and acceptor subunits. As such, the performance of PSC's based upon a wide variety of different push-pull copolymers has been reported and 40 the fundamental understanding of molecular structure-device efficiency relations has strongly increased.¹ Prerequisites for high performance solar cells in terms of the electron donor copolymers are a high extinction coefficient throughout the whole solar emission range and a low-lying HOMO (highest occupied

45 molecular orbital) level. While photon absorption is a determining parameter for the short-circuit current density (J_{sc}), the difference between the HOMO of the electron donor polymer and the LUMO (lowest unoccupied molecular orbital) of the electron acceptor component has been shown to be proportional 50 to the open-circuit voltage (V_{oc}). A sufficiently large LUMO offset is required to provide enough driving force for electron transfer.¹ On the other hand, an increase in the bandgap of the donor copolymer reduces the absorption width. In this respect, there is always a trade-off between V_{oc} and J_{sc} , and fine-tuning of 55 the HOMO/LUMO levels of the push-pull copolymers is imperative to achieve optimal solar cell efficiencies. An attractive approach to optimize the energy levels involves the introduction of electron withdrawing substituents on the conjugated polymer backbone. Fluorination has become a quite general and effective 60 strategy, either on the donor or acceptor building block,^{2,3} resulting in a lowering of both the HOMO and LUMO levels. Combinations of several electron withdrawing groups have also been investigated.⁴

Copolymers composed of alternating N-alkyl-substituted 65 dithieno[3,2-*b*:2',3'-*d*]pyrroles (DTP's) and various electron poor building blocks have been applied in PSC's with limited success, 5,6 mainly due to the high HOMO levels, majorly determined by the electron rich DTP units. These high HOMO levels give rise to rather low V_{oc} 's and consequently, although J_{sc} 's as high as 14.9 70 mA cm⁻² have been observed for DTP-*alt*-DPP copolymers,^{6b} the highest PCE to be reported was only 2.8%.^{6a,h} On the other hand, the DTP fused heterocyclic system also has a few important

strengths. It is readily accessible and copolymers with thiophene have shown high charge carrier mobilities in field-effect transistors (FET's), despite being amorphous.⁷ Dye-sensitized solar cells based on DTP materials have shown excellent performances as well,⁸ and recently small molecule organic solar cells based on N-alkyl-DTP have afforded up to 4.8% efficiency.^{7,9}

In 2010, Rasmussen and co-workers reported the synthesis of N-acyl-substituted DTP's,¹⁰ offering a novel pathway to lower the HOMO levels. In the presented work we have employed this strategy towards the synthesis of alternating low bandgap copolymers, combining N-acyl-DTP's with variable side chain patterns with a number of different acceptor derivatives. For the solar cells based on these copolymers (in combination with PC₇₁BM) the V_{oc} was effectively enhanced (up to 0.80 V), enabling to obtain a record solar cell efficiency of 4.0% for DTP-based copolymers. By spin-coating an additional very thin conjugated polyelectrolyte (CPE) layer on top of the active layer,¹¹ the short-circuit current density was further increased, leading to a maximum PCE of 5.8%.

Results and discussion

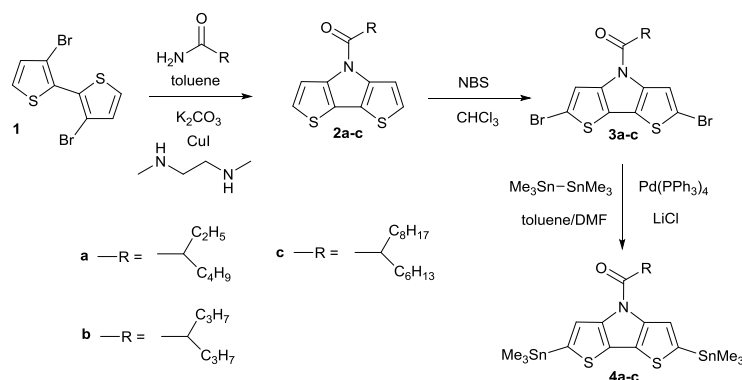
Synthesis and characterization

For the construction of the low bandgap copolymers, the Stille polycondensation reaction was chosen, combining distannylated N-acyl-substituted DTP's and several dibrominated acceptor derivatives. The required bis(trimethylstannyl)-N-acyl-DTP's **4a-c** were synthesized by Stille cross-coupling of hexamethylditin and dibrominated DTP precursors **3a-c** (Scheme 1), prepared by a literature procedure.^{10,12} This protocol consists of a copper catalyzed tandem reaction¹³ of an alkyl amide and 3,3'-dibromo-2,2'-bithiophene (**1**)¹⁴ to obtain DTP's **2a-c**, followed by dibromination with N-bromosuccinimide (NBS). Three different alkyl side chain patterns were introduced to optimize polymer solubility, taking into account the side chain decoration of the acceptor building blocks, and final active layer blend morphology. Synthesis of 2-ethylhexanamide¹⁵ and 2-propylpentanamide¹⁶ was done according to literature and 2-hexyldecanamide was synthesized via a similar approach. As the purity of the bisstannyl-DTP monomers is of crucial importance for the correct stoichiometric balance in the polycondensation reactions to enable the formation of high molar mass materials, and the monomers (oily substances) cannot be crystallized,

recycling (preparative) size exclusion chromatography (SEC) was applied for monomer purification. In this way, residual amounts of monostannylated DTP and DTP oligomers were readily removed. Due to side reactions and the aim for high purity, the yields for the final stannylation step were moderate (39–55 %).

Dibrominated acceptors 4,7-dibromo-2,1,3-benzothiadiazole (BT **5**),¹⁷ 2,5-bis-[5'-bromo-3'-(2''-ethylhexyl)thiophen-2'-yl]thiazolo[5,4-d]thiazole (DTTzTz **6**),¹⁸ and 4,7-bis[5'-bromo-4'-(2''-ethylhexyl)thiophen-2'-yl]-5,6-difluoro-2,1,3-benzothiadiazole (DTBT **7**)¹⁹ were synthesized according to literature procedures, whereas 1,3-dibromo-5-(2'-ethylhexyl)-4H-thieno[3,4-c]pyrrole-4,6(5H)-dione (TPD **8**) was purchased from Sigma-Aldrich and purified by preparative SEC prior to use. The Stille polycondensation reactions were performed under standard conditions (2.5 mol% Pd₂dab₃, 10 mol% P(*o*-tolyl)₃, toluene/DMF, 105 °C, 1 h; Scheme 2) and the crude polymer materials were isolated upon precipitation in ice-cold methanol. No end-capping procedures were applied. The low molar mass fractions were removed by sequential Soxhlet extractions. The copolymers **PDTP-DTTzTz-c** and **PDTP-TPD-c** were readily soluble in chloroform. For **PDTP-BT-c** a fraction soluble in (hot) chlorobenzene was isolated by Soxhlet extraction. However, a large insoluble fraction remained in the Soxhlet tumbler. **PDTP-DTBT-b** dissolved in (hot) *o*-dichlorobenzene only and for **PDTP-DTTzTz-a** no suitable solvent was found. In general, the solubility of the synthesized copolymers is lower as compared to the N-alkyl-DTP analogues (for example, the copolymer *N*-1-pentylhexyl-DTP-*alt*-BT was reported to be readily soluble in common organic solvents,^{6a} whereas **PDTP-BT-c** has a very low solubility).

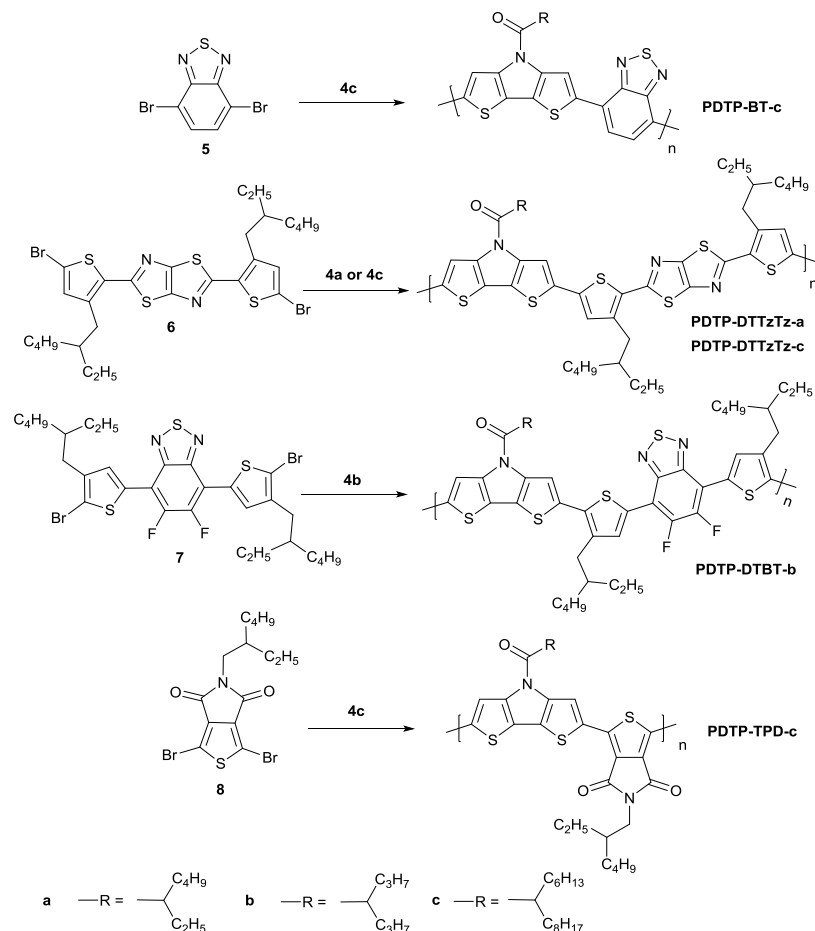
The apparent molar masses of the polymers were determined by SEC relative to polystyrene standards (Table 1). As expected, the *M_n* of the soluble fraction of **PDTP-BT-c** was rather low (7.6 kg mol⁻¹), but for the **PDTP-DTTzTz-c** and **PDTP-TPD-c** materials bearing long branched alkyl side chains reasonably high molar masses were obtained (28 and 29 kg mol⁻¹, respectively). Since polymer chain length and purity are important factors determining solar cell performance,^{1,20} the low and high molar mass fractions of **PDTP-TPD-c** were separated by preparative SEC to yield a **PDTP-TPD-c-H** fraction with an *M_n* of 69 kg mol⁻¹ (see Fig. S1 for chromatograms prior and after preparative SEC). Fractionation of **PDTP-DTTzTz-c** was hindered by its strong aggregation in chloroform and *o*-dichlorobenzene.



Scheme 1 Synthesis of distannylated N-acyl-DTP monomers **4a-c**.

Cite this: DOI: 10.1039/c0xx00000x

www.rsc.org/xxxxxx



Scheme 2 Polymerization of N-acyl-DTP monomers **4a-c** with various acceptors by Stille cross-coupling (similar reaction conditions for all polymerizations: 2.5 mol% Pd₂dba₃, 10 mol% P(*o*-tolyl)₃, toluene/DMF, 105 °C, 1 h; a, b and c denote the alkyl side chain patterns).

Photophysical and electrochemical properties

UV-Vis absorption spectra in solution and thin film were recorded for all copolymers (Fig. 1). All polymers have a broad absorption in the visible region and **PDTP-BT-c** and **PDTP-DTBT-b** also absorb in the UV range. Upon transition from solution to film, a broad shoulder around 760 nm appears in the spectrum of **PDTP-BT-c**, and the absorption maximum shifts from 632 to 651 nm. The **PDTP-DTTzTz-c** material shows a larger optical bandgap, in accordance with the electrochemical data (*vide infra*, Table 1). The wavelength at maximum absorption for **PDTP-DTTzTz-c** shows only a slight red shift from 572 nm to 580 nm upon transition to film, probably because the polymer is already strongly aggregated in chloroform solution. A similar behaviour was previously observed for a 4*H*-cyclopenta[2,1-*b*:3,4-*b'*]dithiophene-*alt*-dithienylthiazolo[5,4-*d*]thiazole (**PCPDT-DTTzTz**) copolymer.^{20a} This is consistent

with the observation that filtration over a 0.45 μm filter renders a colourless filtrate. **PDTP-DTBT-b** behaves similar since no substantial red shift is observed between the spectra in solution and film. Finally, **PDTP-TPD-c** does show a significant red shift of the absorption maxima in thin film (from 610 and 666 nm to 644 and 685 nm, respectively). The relative intensity of the absorption band at higher wavelength slightly increases as well. The electrochemical properties of the polymers were investigated by cyclic voltammetry (CV) and HOMO and LUMO energy levels were determined from the onset of the first oxidation and reduction peaks, respectively (see Table 1). The HOMO levels of all polymers are comparable, except for **PDTP-TPD-c**, which has a substantially deeper HOMO. If one compares these values to the previously reported HOMO energies for analogous N-alkyl-substituted DTP copolymers 'alkyl-PDTP-BT'^{6a} and 'alkyl-PDTP-TPD'^{6c-e} (Table 1 and Fig. S2), it is clear that the HOMO's of **PDTP-BT-c** and **PDTP-TPD-c** are lowered substan-

Cite this: DOI: 10.1039/c0xx00000x

www.rsc.org/xxxxxx

PAPER

Table 1 SEC, UV-Vis and CV data of the DTP-*alt*-acceptor copolymers and a comparison between their experimental and DFT-calculated frontier orbital energies

Polymer	Experimental					Calculated [§]			
	M_n^a (kg mol ⁻¹)	D^a	$E_{g,opt}$ (eV)	HOMO ^b (eV)	LUMO ^b (eV)	Structure	HOMO (eV)	LUMO (eV)	Torsion angle ^h
PDTP-BT-c	7.6 ^c	1.1	1.36	-5.27	-3.38	DA (DADA)	-5.82 (-5.44)	-2.53 (-2.77)	8.9
PDTP-DTTzTz-a	\ ^d	\ ^d	\ ^d	\ ^d	\ ^d	DA (DADA)	-5.58 (-5.36)	-2.26 (-2.50)	19.0, 2.0
PDTP-DTTzTz-c	28	2.4	1.81	-5.27	-3.08				
PDTP-DTBT-b	\ ^d	\ ^d	1.48	-5.21	-3.31	DA (DADA)	-5.60 (-5.41)	-2.66 (-2.77)	37.0, 14.2
PDTP-TPD-c	29	2.1	1.62	-5.39	-3.31	DA (DADA)	-5.93 (-5.63)	-2.26 (-2.64)	3.1
PDTP-TPD-c-H^c	69	1.9	\	\	\				
Alkyl-PDTP-TPD (Lit.)	\	\	\	-5.09 ^f	-3.42 ^f	DA	-5.69	-2.04	\

^a Determined by SEC in THF at 40 °C, ^b Determined by CV, ^c Determined by SEC in chlorobenzene at 60 °C, ^d Not measured due to low solubility, ^e High molar mass fraction isolated by preparative SEC. ^f Experimental values from literature (ref. 6c-e). [§] For the calculations, the alkyl side chains were replaced by methyl groups. ^h The values correspond to the deviation with respect to planarity; the first value is the average inter-DA torsion angle of the DADA structures, whereas the second (if given) is the average intra-acceptor torsion angle.

tially (by 0.46 and 0.30 eV, respectively) due to the introduction of the N-acyl groups.

DFT calculations

To analyze the interactions between the donor and acceptor moieties of the polymers and their impact on the positions of the HOMO and LUMO levels, density functional theory (DFT) calculations were performed using the M05²¹ exchange-correlation functional and the 6-311G(d) basis set. The effects of the solvent (THF) were taken into account within the integral equation formalism of the polarizable continuum model (IEF-PCM).²² All calculations were carried out using Gaussian09.²³ First, the ground state geometries were fully optimized for the individual donor and acceptor moieties as well as for the donor-acceptor combinations (DA). Several conformations differing by the torsion angle between the donor and acceptor units have been considered and the most stable ones were selected to perform calculations on the dimers of donor-acceptor units (DADA). In the calculations, the large alkyl chains were substituted by methyl groups, which accelerates the calculations without impacting the results. Using the optimized geometries, the energies and the topologies of HOMO and LUMO were determined (Table 1). The experimental trends are confirmed by the calculations, i.e. i) **PDTP-TPD** has the lowest-energy HOMO, whereas the other N-acyl-DTP-based materials exhibit similar HOMO energies (most clear for the DADA systems), ii) **PDTP-DTTzTz** has the highest LUMO, and iii) replacing the alkyl by an acyl substituent stabilizes the HOMO by about 0.3 eV. The lowest HOMO of **PDTP-TPD** can be explained by referring to two effects: i) the larger the difference between the HOMO's of the donor and acceptor moieties, the smaller the splitting of the HOMO levels and therefore the lower the HOMO of the DA and DADA oligomers, and ii) in case of similar energy levels, larger torsion angles - between the donor and acceptor pairs or, for **PDTP-DTTzTz** and **PDTP-DTBT**, inside the acceptor - lead to smaller

splitting and lower HOMO. So, the HOMO of the TPD acceptor (-7.67 eV) of **PDTP-TPD** is much lower than the HOMO of the N-acyl-DTP moiety (-6.01 eV), which gives a HOMO for the DA unit of -5.93 eV (i.e. close to the DTP donor unit). On the contrary, the splitting of the HOMO levels in **PDTP-DTTzTz** is larger since the HOMO of the DTTzTz acceptor is located at -5.87 eV (closer to the HOMO of the N-acyl-DTP moiety). Consequently, the HOMO of the DA unit goes up to -5.58 eV. Moreover, when going from the N-alkyl to the N-acyl derivatives, the stabilization of the HOMO of the oligomers results from a stabilization of the HOMO of the donor by 0.30 eV. Finally, as shown in Fig. 2, the delocalization of the HOMO over the whole system, and therefore the size of the units and the amplitude of the torsion angles, plays also a role on the evolution of the frontier orbital levels as a function of system size, going from DA to DADA.

Photovoltaic properties

To evaluate their photovoltaic properties, the N-acyl-DTP-based copolymers were blended with PC₇₁BM and applied as photoactive layers in BHJ organic solar cells with a standard configuration (glass:ITO:PEDOT:PSS:active layer:Ca:Al, Table 2 and Fig. 3). The low solubility of **PDTP-BT-c** and **PDTP-DTBT-b** impeded smooth processing and lead to poor active layer film quality and very low PCE's. For the devices with **PDTP-DTTzTz-c:PC₇₁BM** (1:3 optimized ratio) active layer blends spin-coated from chlorobenzene (CB), a V_{oc} of 0.64 V was obtained (PCE 2.47%), which is rather high when compared to most N-alkyl-DTP based copolymers.^{5,6} This is consistent with both the experimentally and theoretically derived deepened HOMO levels due to the introduction of the N-acyl groups. By using 1-chloronaphthalene (CN) as a processing additive, the J_{sc} and fill factor (FF) were increased by approximately 10% and a PCE of 3.29% was obtained (Fig. 3, Table 2).

Cite this: DOI: 10.1039/c0xx00000x

www.rsc.org/xxxxxx

PAPER

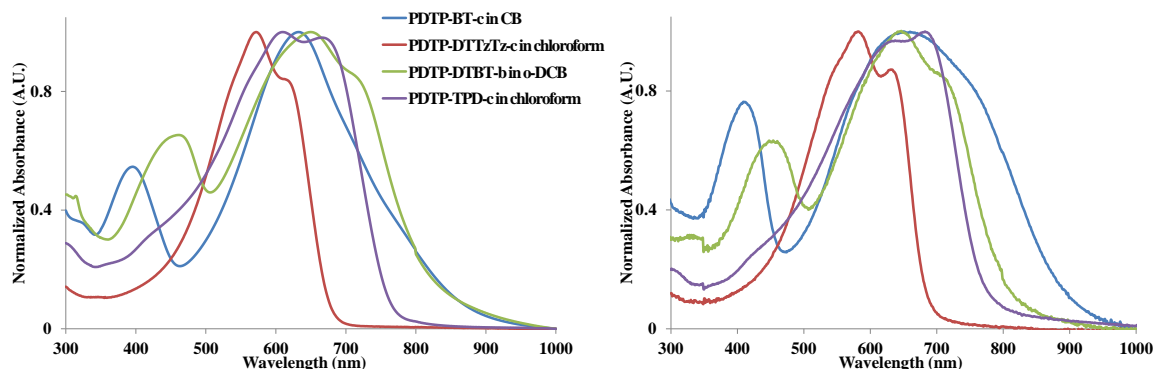


Fig. 1 UV-Vis absorption spectra for all soluble DTP-based copolymers in solution (left) and thin film (right; same colour code)

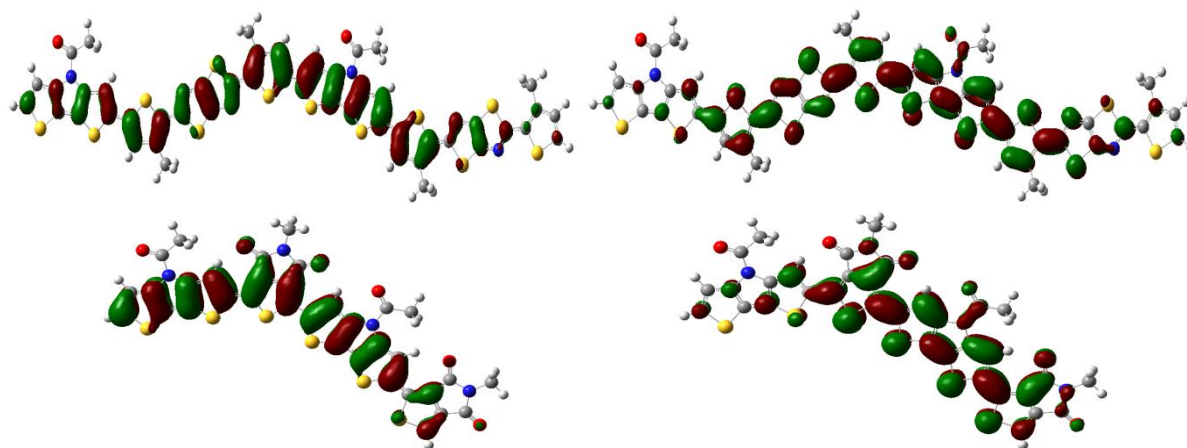


Fig. 2 Sketch of the HOMO (left) and LUMO (right) of PDTP-DTTzTz (top) and PDTP-TPD (bottom) for the most stable conformer (isosurfaces of 0.02 a.u.; DADA oligomers).

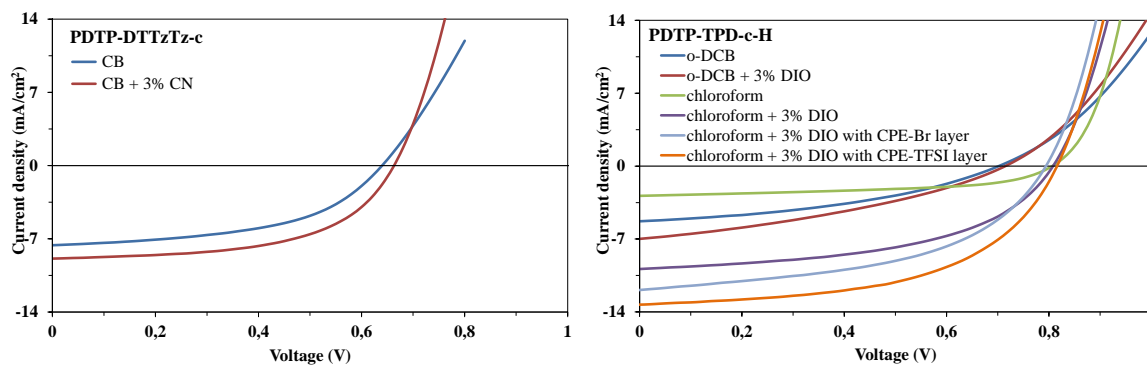


Fig. 3 J-V curves of PSC's with PDTP-DTTzTz-c:PC₇₁BM (left) or PDTP-TPD-c-H:PC₇₁BM (right) photoactive layers processed from different solvents.

Cite this: DOI: 10.1039/c0xx00000x

www.rsc.org/xxxxxx

PAPER

The combination of TPD with various donor units has already been reported to lead to excellent solar cell performances and improved V_{oc} 's.^{6c-e,24} As the **PDTP-TPD** copolymer showed the lowest HOMO value amongst the series, this material was thought to have the most promising characteristics to afford high solar cell efficiencies. TPD was combined with N-acyl-DTP **4c** decorated with the longest branched alkyl side chain to ensure good solubility. Furthermore, the obtained crude polymer (after Soxhlet extractions) was further purified and fractionated by preparative SEC, which was previously shown to be an effective means to enhance solar cell performance (by improving material purity and increasing M_n).²⁰ Processing **PDTP-TPD-c-H:PC₇₁BM** (1:3 optimized ratio) blends from *o*-dichlorobenzene (*o*-DCB) resulted in devices with an open-circuit voltage of 0.70 V and blends in chloroform afforded an even higher V_{oc} of 0.80 V, the highest value reported for DTP-based copolymers to date. Addition of a processing additive (1,8-diiodooctane or DIO) again resulted in an increase in J_{sc} , which was most pronounced for chloroform as a solvent. In this case, the J_{sc} increased quite drastically (by a factor 3.5 up to 9.88 mA cm⁻²), without affecting the FF and V_{oc} , giving rise to a PCE of 4.04% (Fig. 3, Table 2). The external quantum efficiency (EQE) was determined for the best performing devices (Fig. 4), showing the PC₇₁BM contribution at shorter wavelengths and a polymer contribution up to ~650 or 750 nm for **PDTP-DTTzTz-c** and **PDTP-TPD-c-H**, respectively, in accordance with the UV-Vis absorption spectra.

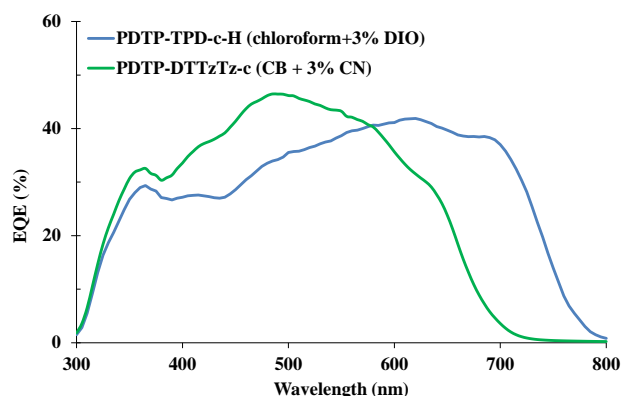


Fig. 4 EQE spectra for the best performing PSC devices.

The influence of the processing additives can be related to an optimized BHJ blend morphology, as clearly evidenced by AFM imaging.^{1f,6g} The thin film topography of the active layers as investigated by PeakForce AFM showed (similar) large scale phase segregation if no processing additive was employed (Fig. 5). From these images, characteristic spherical structures can be observed, for which the calculated surface coverage was found to be ~70–75%. Additionally, the obtained layers were subjected to

conductive AFM (C-AFM) under positive and negative sample bias (Fig. S3). When applying a positive bias, the spherical shapes showed conductivity, which was absent under negative bias. The opposite holds true for the space around the spherical shapes.²⁵ This confirms the idea that these spherical structures consist mainly of PC₇₁BM, and that the polymer rather forms the surrounding matrix. A similar topography has been described for other DTP-based materials.^{6f-g} The observed large phase segregation is unfavourable for solar cell performance since it leads to a reduced interfacial area between PC₇₁BM and copolymer, necessary for efficient charge separation. It is well known that processing additives can greatly suppress the size of these phase-segregated domains.^{1f} Through the addition of a small amount of CN (for **PDTP-DTTzTz-c**) or DIO (for **PDTP-TPD-c-H**), a strong improvement in blend (nano)morphology could be obtained (Fig. 5). This phenomenon was confirmed by C-AFM images under positive and negative bias showing a uniform conductance (Fig. S3).

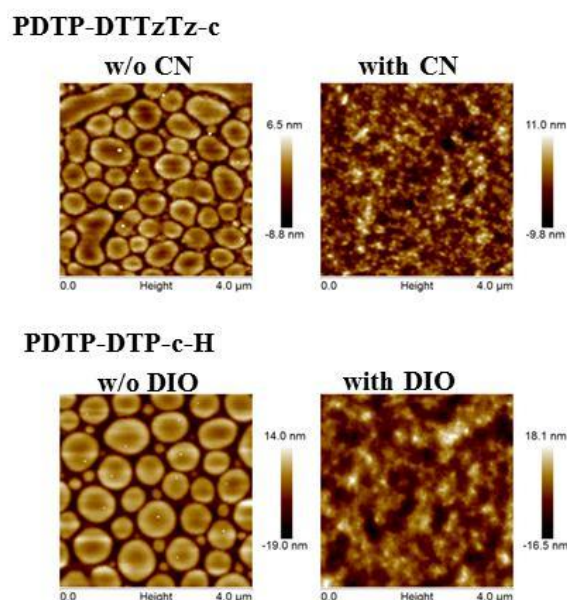


Fig. 5 Topographic PeakForce tapping mode AFM images of spin-coated films of **PDTP-X** and PC₇₁BM (measurements on solar cell devices).

Finally, to enhance the PCE of the **PDTP-TPD-c-H:PC₇₁BM** PSC's even further, an additional CPE interlayer^{26,27} was spin-coated between the active layer and the Al top electrode (replacing the oxidatively labile Ca layer). In previous work, we have introduced imidazolium-substituted ionic polythiophenes as effective cathode interlayer materials pushing up the efficiencies of polymer solar cells, mainly by increasing the short-circuit current.^{11,28} The addition of a thin cathode interlayer is generally believed to induce an aligned interphase dipole, reducing contact

Cite this: DOI: 10.1039/c0xx00000x

www.rsc.org/xxxxxx

Table 2 Photovoltaic performances of N-acyl-DTP-based BHJ polymer solar cell devices.

Layer sequence ^a	Processing solvent	V _{oc} (V)	J _{sc} (mA cm ⁻²)	FF	Best PCE (%)	Average PCE ^b (%)
PDTP-DTTzTz-c :PC ₇₁ BM/Ca/Al	CB	0.64	7.61	0.51	2.47	2.31
PDTP-DTTzTz-c :PC ₇₁ BM/Ca/Al	CB + 3% (v/v) CN	0.66	8.89	0.56	3.29	3.09
PDTP-TPD-c-H :PC ₇₁ BM/Ca/Al	<i>o</i> -DCB	0.70	5.30	0.39	1.46	1.17
PDTP-TPD-c-H :PC ₇₁ BM/Ca/Al	<i>o</i> -DCB + 3% (v/v) DIO	0.72	6.99	0.35	1.74	1.65
PDTP-TPD-c-H :PC ₇₁ BM/Ca/Al	CHCl ₃	0.80	2.85	0.52	1.20	1.15
PDTP-TPD-c-H :PC ₇₁ BM/Ca/Al	CHCl ₃ + 3% (v/v) DIO	0.80	9.88	0.51	4.04	3.74
PDTP-TPD-c-H :PC ₇₁ BM/CPE-Br/Al	CHCl ₃ + 3% (v/v) DIO	0.82	12.35	0.50	5.40	5.01
PDTP-TPD-c-H :PC ₇₁ BM/CPE-TFSI/Al	CHCl ₃ + 3% (v/v) DIO	0.82	13.30	0.53	5.82	5.42

^a 1:3 polymer:fullerene ratio. ^b Averages over 4–8 devices.

resistance and affording more efficient charge extraction from the active layer to the top electrode. Two different CPE's, differing by their composition (homo- vs copolymer), side chain patterns and counter ions (Br and TFSI,²⁸ see Fig. S4), were applied on top of **PDTP-TPD-c**:PC₇₁BM active layers to investigate their influence on the I-V characteristics. As shown in Table 2 and Fig. 3 (EQE's in Fig. S5), this resulted in a substantial increase of the J_{sc} for both cases (with smaller effects on V_{oc} and FF). The effect was most pronounced for the **CPE-TFSI** interlayer, with a noticeable increase in J_{sc} of ~35% (up to 13.3 mA cm⁻²), leading to a final PCE of 5.82%.

Conclusions

In summary, N-acyl-DTP's have been identified as attractive building blocks for light-harvesting low bandgap copolymers for organic photovoltaics. The open-circuit voltage of polymer solar cells derived from N-acyl-substituted DTP-*alt*-acceptor copolymers is notably higher than previously observed for the N-alkyl-DTP analogues, with **PDTP-TPD** showing the highest V_{oc} (0.80 V) among the series. Consequently, the solar cell efficiencies are significantly higher than for the best performing N-alkyl-substituted DTP-based polymer donor material reported so far (PCE of 2.8%).^{6a,h} N-acyl-substitution of DTP is hence an effective approach to an increased V_{oc} for polymer solar cells. Moreover, the solar cell efficiencies were further enhanced by the addition of a conjugated polyelectrolyte cathode interlayer, mainly by an increase in short-circuit current, up to a PCE of 5.82%. Further improvements are currently pursued by continued energy level tailoring, variation of the (N-acyl-DTP) side chain pattern and device optimization.²⁹

Experimental section

Materials and instruments

Unless stated otherwise, all reagents and chemicals were obtained from commercial sources and used without further purification. 1,3-Dibromo-5-(2'-ethylhexyl)-4H-thieno[3,4-*c*]pyrrole-4,6(5H)-dione (TPD **8**) (Sigma-Aldrich, 97 %) was purified by preparative

SEC prior to use. Preparative (recycling) SEC was performed on JAIGEL 1H and 2H columns attached to an LC system equipped with a UV detector (path 0.5 mm) and a switch for recycling and collecting the eluent (CHCl₃; flow rate 3.5 mL min⁻¹, injection volume 3.0 mL). Solvents were dried by a solvent purification system (MBraun, MB-SPS-800) equipped with alumina columns. NMR chemical shifts (δ, in ppm) were determined relative to the residual CHCl₃ (7.26 ppm) or CDHCl₂ (5.32 ppm) signals or the ¹³C resonance shift of CDCl₃ (77.16 ppm). For the N-acyl-substituted DTP's quantitative ¹³C NMR measurements were obtained with chromium(III) acetylacetonate as a relaxation agent. High resolution electrospray ionization-mass spectrometry (ESI-MS) was performed using an LTQ Orbitrap Velos Pro mass spectrometer equipped with an atmospheric pressure ionization source operating in the nebulizer assisted electrospray mode. The instrument was calibrated in the m/z range 220–2000 using a standard solution containing caffeine, MRFA and Ultramark 1621. UV-Vis measurements were performed on a VARIAN Cary 5000 UV-Vis-NIR spectrophotometer with a scan rate of 600 nm min⁻¹. The films for the UV-Vis measurements were prepared by drop-casting the polymer solutions (**PDTP-BT-c** in chlorobenzene, **PDTP-DTBT-b** in (warm) *o*-dichlorobenzene, and **PDTP-DTTzTz-c** and **PDTP-TPD-c** in chloroform) on a quartz substrate. The solid-state UV-Vis spectra were used to estimate the optical band gaps (from the wavelength at the intersection of the tangent drawn at the low energy side of the absorption spectrum with the x-axis; E_g (eV) = 1240/(wavelength in nm)). FT-IR spectra of 2-hexyldecanamide and dibrominated DTP's **3a-c** were recorded as thin films on a NaCl disk with a Bruker Tensor 27 from 1000 to 4000 cm⁻¹. Analysis of the molar masses and molar mass distributions of the polymers was performed on a Tosoh EcoSEC System comprising of an autosampler, a PSS guard column SDV (50 x 7.5 mm), followed by three PSS SDV analytical linear XL columns (5 μm, 300 x 7.5 mm), a differential refractive index detector (Tosoh EcoSEC RI) and a UV-detector (254 nm) using THF as the eluent at 40 °C with a flow rate of 1.0 mL min⁻¹. In particular cases (due to solubility issues) a Spectra Series P100 (Spectra Physics) pump equipped with two mixed-B columns (10 μm, 2 x 30 cm, Polymer

Laboratories) and an Agilent 1100 DAD UV detector (600 nm) was applied with chlorobenzene as an eluent at 60 °C and a flow rate of 1.0 mL min⁻¹. Both systems were calibrated using linear narrow polystyrene standards. Electrochemical measurements (cyclic voltammetry) were performed with an Eco Chemie Autolab PGSTAT 30 potentiostat/galvanostat using a three-electrode microcell with a Pt working electrode, a Pt counter electrode and a Ag/AgNO₃ reference electrode (Ag wire dipped in a solution of 0.01 M AgNO₃ and 0.1 M NBu₄PF₆ in anhydrous acetonitrile). The reference electrode was calibrated against ferrocene/ferrocenium as an external standard. Samples were prepared by dip-coating the Pt working electrode in the respective polymer solutions (also used for the film preparation for solid-state UV-Vis). The CV measurements were done on the resulting films with 0.1 M NBu₄PF₆ in anhydrous acetonitrile as the electrolyte solution. To prevent air from entering the system, the experiments were conducted under a curtain of Ar. Cyclic voltammograms were recorded at a scan rate of 100 mV s⁻¹. The HOMO-LUMO frontier energy levels were determined using the onset potentials for oxidation and reduction, referenced to ferrocene/ferrocenium, which is estimated to have an oxidation potential of -4.98 eV vs. vacuum.

Monomer synthesis

2-Hexyldecanamide

A mixture of 2-hexyldecanoic acid (8.28 g, 32.3 mmol) and SOCl₂ (2.93 mL, 40.4 mmol) was refluxed for 30 min and subsequently added drop wise to an ice-cold ammonia solution (32% in H₂O; 25.8 mL). The resulting precipitate was filtered off, washed with H₂O and recrystallized from MeOH, yielding a white solid (6.13 g, 74 %). δ_{H} (400 MHz, CDCl₃): 5.82 (br, 1H), 5.70 (br, 1H), 2.16–2.06 (m, 1H), 1.64–1.51 (m, 2H), 1.48–1.37 (m, 2H), 1.36–1.18 (m, 20H), 0.90–0.84 (m, 6H), δ_{C} (100 MHz, CDCl₃): 179.2 (CO), 47.4, 33.2, 32.0, 31.8, 29.8, 29.6, 29.5, 29.4, 27.7, 22.7, 14.3, HRMS: Calcd. for C₁₆H₃₄NO [M+H]⁺: 256.2562, found: 256.2651, FT-IR: ν_{max} /cm⁻¹ 3370, 3181, 2952, 2920, 2851, 1655, 1465, 1423, 1319, 1284, 1147, 1134.

N-acyl-substituted DTP's **3a-c** were prepared according to literature procedures.^{10,12}

N-(2-Ethylhexanoyl)dithieno[3,2-*b*:2',3'-*d*]pyrrole (**2a**)

Green solid (1.642 g, 44%), δ_{H} (400 MHz, CD₂Cl₂): 8.10–7.00 (br, 2H), 7.28 (d, *J* = 5.3 Hz, 2H), 3.40–3.28 (m, 1H), 1.98–1.84 (m, 2H), 1.80–1.62 (m, 2H), 1.42–1.25 (m, 4H), 0.97 (t, *J* = 7.4 Hz, 3H), 0.87 (t, *J* = 7.1 Hz, 3H), δ_{C} (100 MHz, CDCl₃): 173.0 (1C), 143.3 (1C), 140.5 (1C), 124.3 (2C), 121.4 (2C), 118.0 (1C), 115.5 (1C), 46.0 (1C), 31.1 (1C), 29.4 (1C), 24.9 (1C), 22.9 (1C), 14.0 (1C), 11.6 (1C), HRMS: Calcd. for C₁₆H₂₀NOS₂ [M+H]⁺: 306.0908, found: 306.0991.

2,6-Dibromo-*N*-(2-ethylhexanoyl)dithieno[3,2-*b*:2',3'-*d*]pyrrole (**3a**)

White solid (1.708 g, 71%), δ_{H} (400 MHz, CD₂Cl₂): 7.60 (br, 2H), 3.20–3.11 (m, 1H), 1.95–1.81 (m, 2H), 1.78–1.60 (m, 2H), 1.38–1.23 (m, 4H), 0.95 (t, *J* = 7.4 Hz, 3H), 0.90–0.84 (m, 3H), δ_{C} (100 MHz, CDCl₃): 172.6 (1C), 139.7 (1C), 137.5 (1C), 121.0 (3C), 118.7 (1C), 111.6 (2C), 46.0 (1C), 30.9 (1C), 29.3 (1C), 24.9 (1C), 22.9 (1C), 13.9 (1C), 11.4 (1C), HRMS: Calcd for C₁₆H₁₇Br₂NOS₂ [M]⁺: 462.9098, found: 462.9114, FT-IR: ν_{max} /cm⁻¹ 3126, 2959, 2930, 2871, 1709, 1491, 1458, 1383, 1267,

1233, 1169, 1092, 1033.

2,6-Bis(trimethylstannyl)-*N*-(2-ethylhexanoyl)dithieno[3,2-*b*:2',3'-*d*]pyrrole (**4a**)

A solution of dibromo-DTP **3a** (0.450 g, 0.971 mmol) in dry toluene (2 mL) was added to a mixture of hexamethylditin (1.34 g, 4.08 mmol), LiCl (0.247 g, 5.83 mmol) and Pd(PPh₃)₄ (56 mg, 0.049 mmol) in dry toluene (4 mL). The resulting mixture was purged with N₂ for 10 min and subsequently heated to 105 °C. After 1 h the mixture was allowed to cool down to room temperature and diethyl ether and water were added. The organic layer was washed with water and dried over Na₂SO₄. Purification of the crude product by preparative SEC yielded a pale yellow oil (0.338 g, 55%). δ_{H} (300 MHz, CD₂Cl₂): 7.76 (br, 1H), 7.28 (br, 1H), 3.31 (quint, *J* = 6.0 Hz, 1H), 1.95–1.80 (m, 2H), 1.78–1.57 (m, 2H), 1.40–1.21 (m, 4H), 0.95 (t, *J* = 7.4 Hz, 3H), 0.86 (t, *J* = 7.1 Hz, 3H), 0.40 (s, 18H).

N-(2-Propylpentanoyl)dithieno[3,2-*b*:2',3'-*d*]pyrrole (**2b**)

Viscous colorless oil (0.958 g, 27%), δ_{H} (400 MHz, CD₂Cl₂): 7.90–7.10 (br, 2H), 7.26 (d, *J* = 5.3 Hz, 2H), 3.43–3.34 (m, 1H), 1.92–1.77 (m, 2H), 1.70–1.57 (m, 2H), 1.42–1.30 (m, 4H), 0.88 (t, *J* = 7.3 Hz, 6H), δ_{C} (100 MHz, CDCl₃): 173.1 (1C), 143.4 (1C), 140.4 (1C), 124.3 (2C), 121.5 (2C), 117.9 (1C), 115.4 (1C), 44.3 (1C), 34.1 (2C), 20.4 (2C), 14.2 (2C), HRMS: Calcd. for C₁₆H₁₉NOS₂Na [M+Na]⁺: 328.0800, found: 328.0812.

2,6-Dibromo-*N*-(2-propylpentanoyl)dithieno[3,2-*b*:2',3'-*d*]pyrrole (**3b**)

White solid (0.993 g, 91%), δ_{H} (300 MHz, CD₂Cl₂): 7.56 (br, 2H), 3.28–3.17 (m, 1H), 1.92–1.75 (m, 2H), 1.71–1.52 (m, 2H), 1.45–1.22 (m, 4H), 0.88 (t, *J* = 7.3 Hz, 6H), δ_{C} (100 MHz, CDCl₃): 172.8 (1C), 140.0 (1C), 137.2 (1C), 121.0 (3C), 118.4 (1C), 111.6 (2C), 44.4 (1C), 34.0 (2C), 20.3 (2C), 14.2 (2C), HRMS: Calcd. for C₁₆H₁₇Br₂NOS₂ [M]⁺: 462.9098, found: 462.9116, FT-IR: ν_{max} /cm⁻¹ 3126, 2958, 2930, 2871, 1709, 1491, 1463, 1384, 1357, 1257, 1219, 1169, 1092, 1035.

2,6-Bis(trimethylstannyl)-*N*-(2-propylpentanoyl)dithieno[3,2-*b*:2',3'-*d*]pyrrole (**4b**)

According to the procedure as outlined for **4a**: pale yellow oil (0.263 g 39%), δ_{H} (400 MHz, CD₂Cl₂): 7.81 (br, 1H), 7.27 (br, 1H), 3.46–3.38 (m, 1H), 1.92–1.80 (m, 2H), 1.67–1.58 (m, 2H), 1.46–1.33 (m, 4H), 0.91 (t, *J* = 7.3 Hz, 6H), 0.42 (s, 18H).

N-(2-Hexyldecanoyl)dithieno[3,2-*b*:2',3'-*d*]pyrrole (**2c**)

Beige solid (3.62 g, 58%), δ_{H} (400 MHz, CD₂Cl₂): 7.95–7.15 (br, 2H), 7.28 (d, *J* = 5.3 Hz, 2H), 3.40–3.31 (m, 1H), 1.93–1.81 (m, 2H), 1.72–1.60 (m, 2H), 1.41–1.15 (m, 20H), 0.87–0.81 (m, 6H), δ_{C} (100 MHz, CDCl₃): 173.1 (1C), 143.6 (1C), 140.3 (1C), 124.3 (2C), 121.8 (1C), 121.1 (1C), 118.0 (1C), 115.4 (1C), 44.7 (1C), 31.9 (2C), 31.8 (1C), 31.6 (1C), 29.8 (1C), 29.5 (1C), 29.4 (1C), 29.2 (1C), 27.2 (2C), 22.64 (1C), 22.59 (1C), 14.12 (1C), 14.05 (1C), HRMS: Calcd. for C₂₄H₃₅NOS₂Na [M+Na]⁺: 440.2052, found: 440.2078.

2,6-Dibromo-*N*-(2-hexyldecanoyl)dithieno[3,2-*b*:2',3'-*d*]pyrrole (**3c**)

White solid (4.11 g, 92%), δ_{H} (400 MHz, CD₂Cl₂): 7.79 (br, 1H), 7.37 (br, 1H), 3.25–3.16 (m, 1H), 1.90–1.79 (m, 2H), 1.70–1.59 (m, 2H), 1.37–1.17 (m, 20H), 0.88–0.82 (m, 6H), δ_{C} (100 MHz, CDCl₃): 172.8 (1C), 140.1 (1C), 137.1 (1C), 121.0 (3C), 118.3 (1C), 111.6 (2C), 44.8 (1C), 31.8 (3C), 31.6 (1C), 29.7 (1C), 29.4 (1C), 29.3 (1C), 29.2 (1C), 27.1 (2C), 22.63 (1C), 22.56 (1C),

14.1 (1C), 14.0 (1C), HRMS: calcd. for $C_{24}H_{33}Br_2NOS_2Na$ [M+Na]⁺: 589.0242, found: 589.0257, FT-IR: ν_{max}/cm^{-1} 3127, 2953, 2925, 2854, 1710, 1491, 1464, 1382, 1359, 1240, 1093, 1030.

5 2,6-Bis(trimethylstannyl)-N-(2-hexyldecanoyl)dithieno[3,2-b:2',3'-d]pyrrole (4c)

According to the procedure as outlined for **4a**: pale yellow oil (0.896 g, 46%), ¹H NMR (400 MHz, CD₂Cl₂): 7.82 (br, 1H), 7.24 (br, 1H), 3.43–3.32 (m, 1H), 1.93–1.78 (m, 2H), 1.72–1.58 (m, 10 2H), 1.42–1.17 (m, 20H), 0.88–0.82 (m, 6H), 0.42 (s, 18H).

Polymer synthesis

PDTP-BT-c

A solution of DTP monomer **4c** (255.1 mg, 0.343 mmol) in dry toluene (10 mL) was added drop wise via a syringe to a mixture of 4,7-dibromo-2,1,3-benzothiadiazole (100.9 mg, 342 μ mol), Pd₂dba₃ (7.9 mg, 8.6 μ mol) and P(*o*-tolyl)₃ (10.5 mg, 34.3 μ mol) in dry DMF (2.5 mL) under inert atmosphere. After purging with N₂ for 15 min, the mixture was heated to 105 °C for 1 h. The resulting blue-green solution was added drop wise to ice cold 15 MeOH. The precipitate was filtered off and purified by subsequent Soxhlet extractions with acetone, hexanes, chloroform and chlorobenzene. The chlorobenzene fraction was precipitated in ice-cold MeOH to yield a black solid (28%). ¹H NMR could not be recorded due to the low product solubility. GPC (chlorobenzene, 60 °C, PS standards): $M_n = 7.6 \text{ kg mol}^{-1}$, $D = 1.1$.

PDTP-DTTzTz-a

Similar to the procedure as outlined for **PDTP-BT-c**, but with a solvent mixture DMF:toluene 1:5. After precipitation in MeOH, the polymer could not be redissolved again.

30 PDTP-DTTzTz-c

Similar to the procedure as outlined for **PDTP-BT-c**. Soxhlet extractions were done with acetone, hexanes and chloroform. The chloroform fraction was precipitated in ice-cold MeOH, yielding a black solid (89%). δ_H (400 MHz, CDCl₃) 8.0–5.6 (br, 4H), 3.28 (br, 1H), 2.2–1.0 (br, 46H), 1.0–0.5 (br, 18H), GPC (THF, 40 °C, PS standards): $M_n = 28 \text{ kg mol}^{-1}$, $D = 2.4$.

PDTP-DTBT-b

Similar to the procedure as outlined for **PDTP-BT-c**. Soxhlet extractions were done with acetone, hexanes, chloroform and chlorobenzene. The fraction remaining in the Soxhlet timble was dissolved in *o*-dichlorobenzene under reflux. The resulting solution was concentrated *in vacuo* and added drop wise to ice-cold MeOH, yielding a black solid (62%). Due to the low product solubility, no NMR or GPC could be obtained.

45 PDTP-TPD-c

Similar to the procedure as outlined for **PDTP-BT-c**. Soxhlet extractions were done with acetone, hexanes and chloroform. The chloroform fraction was precipitated in ice-cold MeOH, yielding a black solid (84%). δ_H (400 MHz, CD₂Cl₂): 9.50–8.10 (br, 1H), 50 8.10–6.30 (br, 1H), 4.10–2.80 (br, 3H), 2.50–0.40 (br, 44H), GPC (THF, 40 °C, PS standards): $M_n = 29 \text{ kg mol}^{-1}$, $D = 2.1$.

PSC processing and characterization

BHJ organic solar cells were produced using the standard glass:ITO:PEDOT-PSS:active layer:Ca:Al architecture. ITO 55 (Kintec, 100 nm, 20 Ohm/sq) covered glass substrates were cleaned thoroughly with soap, demineralized water, acetone and isopropanol prior to a UV/O₃ treatment for 15 min. Afterwards,

PEDOT-PSS [poly(3,4-ethylenedioxythiophene)-poly(styrene-sulfonic acid)] was spin-coated at a thickness of approximately 30 nm. The rest of the processing was performed in an inert atmosphere (glove box), starting with an annealing step of 15 min at 130 °C. Consequently, the active layer, consisting of **PDTP-DTTzTz-c:PC₇₁BM** (40 mg mL⁻¹ total conc.) or **PDTP-TPD-c-H:PC₇₁BM** (20 mg mL⁻¹ total conc.), was spin-coated on top at 65 varying thicknesses. As a final step, Ca and Al were deposited under vacuum as top electrodes with thicknesses of 30 and 80 nm, respectively. In this way, an active device area of 3 mm² was obtained. For the devices containing the CPE materials (see structures in Fig. S4), the cathode interlayers were spin-coated on 70 top of the active layer (from a 0.025 w/v% solution in MeOH) before deposition of the Al top electrode.^{11,27b} I-V characteristics were measured using a Newport class A solar simulator (model 91195A) calibrated with a silicon solar cell to give an AM 1.5g solar spectrum. For AFM imaging, a Bruker Multimode 8 AFM 75 was used. C-AFM images were made using Pt/Ir coated probes with a force constant of ~0.4 N m⁻¹ at bias voltages of +5 or -5 V with a maximum deflection setpoint of 0.6 V. EQE measurements were performed with a Newport Apex illuminator (100 W Xenon lamp, 6257) as the light source, a Newport Cornerstone 130° 80 monochromator, and a Stanford SR830 lock-in amplifier for the current measurements. A silicon FDS100-CAL photodiode was employed as a reference cell.

Acknowledgements

The authors gratefully acknowledge financial support from 85 Hasselt University and the IWT (Flemish government agency for Innovation by Science and Technology). The authors further thank BELSPO for funding the IAP 7/05 network. The reported activity is partly supported by the project ORGANEXT (EMR. INT4-1.2.-2009-04/054), selected in the frame of the operational 90 program INTERREG IV-A Euregio Maas-Rijn. The FWO (Research Foundation Flanders) and SIM (Strategisch Initiatief Materialen vzw) are acknowledged for the M.ERA-NET project "RADESOL" (GA.013.13N) and the program "Solution based Processing of Photovoltaic Modules" (SoPPoM, GA n°2010-01, 95 including the projects OPvTECH and absCIGS), respectively. V.L. thanks the F.R.S.-FNRS for his Research Associate position. The calculations were performed on the computing facilities of the Consortium des Équipements de Calcul Intensif (CÉCI), in particular those of the Plateforme Technologique de Calcul 100 Intensif (PTCI) installed in the University of Namur, for which the authors acknowledge financial support of the FNRS-FRFC (Conventions No. 2.4.617.07.F and 2.5020.11) and the University of Namur. We also acknowledge Hercules for providing the funding for the LTQ Orbitrap Velos Pro mass spectrometer.

105 Notes and references

- ^a Design & Synthesis of Organic Semiconductors (DSOS), Institute for Materials Research (IMO-IMOMEC), Hasselt University, Agoralaan 1 - Building D, B-3590 Diepenbeek, Belgium.
^b IMOMEC Assoc. Lab., IMEC, Universitaire Campus - 110 Wetenschapspark 1, B-3590 Diepenbeek, Belgium.
^c Organic & Nanostructured Electronics and Energy (ONE²), Institute for Materials Research (IMO-IMOMEC), Hasselt University, Universitaire Campus - Wetenschapspark 1, B-3590 Diepenbeek, Belgium.

- ^d Laboratoire de Chimie Théorique, University of Namur, Rue de Bruxelles 61, B-5000 Namur, Belgium.
Electronic Supplementary Information (ESI) available: Analytical size exclusion chromatograms, visualization of the HOMO-LUMO energy levels for different DTP-based polymers, PeakForce AFM images, structures of the CPE interlayer materials, EQE spectra for **PDTP-TPD-c-H** with and without CPE interlayers, and ¹H and ¹³C NMR spectra of the copolymers and their precursors. See DOI: 10.1039/b000000x/
- 1 Reviews on polymer-based OPV's: (a) M. Jørgensen, K. Norrman, S. A. Gevorgyan, T. Tromholt, B. Andreasen and F. C. Krebs, *Adv. Mater.*, 2012, **24**, 580; (b) H. Zhou, L. Yang and W. You, *Macromolecules*, 2012, **45**, 607; (c) Y. Li, *Acc. Chem. Res.*, 2012, **45**, 723; (d) Y. Su, S. Lan and K. Wei, *Mater. Today*, 2012, **15**, 554; (e) R. A. J. Janssen and J. Nelson, *Adv. Mater.*, 2013, **25**, 1847; (f) H.-C. Liao, C.-C. Ho, C.-Y. Chang, M.-H. Jao, S. B. Darling and W.-F. Su, *Mater. Today*, 2013, **16**, 326; (g) S. Lizin, S. Van Passel, E. De Schepper, W. Maes, L. Lutsen, J. Manca and D. Vanderzande, *Energy Environ. Sci.*, 2013, **6**, 3136.
- 2 (a) Z. He, C. Zhong, S. Su, M. Xu, H. Wu and Y. Cao, *Nat. Photonics*, 2012, **6**, 591; (b) C. Cabanetos, A. El Labban, J. A. Bartelt, J. D. Douglas, W. M. Mateker, J. M. Fréchet, M. D. McGehee and P. M. Beaujuge, *J. Am. Chem. Soc.*, 2013, **135**, 4556; (c) M. Zhang, X. Guo, S. Zhang and J. Hou, *Adv. Mater.*, 2014, **26**, 1118.
- 3 (a) Z. Li, J. Lu, S.-C. Tse, J. Zhou, X. Du, Y. Tao and J. J. Ding, *J. Mater. Chem.*, 2011, **21**, 3226; (b) Y. Zhang, S.-C. Chien, K.-S. Chen, H.-L. Yip, Y. Sun, J. A. Davies, F.-C. Chen and A. K.-Y. Jen, *Chem. Commun.*, 2011, **47**, 11026; (c) S. Albrecht, S. Janietz, W. Schindler, J. Frisch, J. Kurpiers, J. Kniepert, S. Inal, P. Pingel, K. Fostropoulos, N. Koch and D. J. Neher, *J. Am. Chem. Soc.*, 2012, **134**, 14932; (d) H. Chang, C. Tsai, Y. Lai, D. Chiou, S. Hsu, C. Hsu and Y. Cheng, *Macromolecules*, 2012, **45**, 9282; (e) T. Umeyama, Y. Watanabe, E. Douvogianni and H. J. Imahori, *J. Phys. Chem. C*, 2013, **117**, 21148; (f) H. Bronstein, J. M. Frost, A. Hadipour, Y. Kim, C. B. Nielsen, R. S. Ashraf, B. P. Rand, S. Watkins and I. McCulloch, *Chem. Mater.*, 2013, **25**, 277; (g) A. C. Stuart, J. R. Tumbleston, H. Zhou, W. Li, S. Liu, H. Ade and Y. Wei, *J. Am. Chem. Soc.*, 2013, **135**, 1806; (h) L. Xiao, B. Liu, X. Chen, Y. Li, W. Tang and Y. Zou, *RSC Adv.*, 2013, **3**, 11869; (i) W. Zhuang, H. Zhen, R. Kroon, Z. Tang, S. Hellström, L. Hou, E. Wang, D. Gedefaw, O. Inganäs, F. Zhang and M. R. Andersson, *J. Mater. Chem. A*, 2013, **1**, 13422.
- 4 (a) H. Chen, J. Hou, S. Zhang, Y. Liang, G. Yang, Y. Yang, L. Yu, Y. Wu and G. Li, *Nat. Photonics*, 2009, **3**, 649; (b) Y. Huang, L. Huo, S. Zhang, X. Guo, C. C. Han, Y. Li and J. Hou, *Chem. Commun.*, 2011, **47**, 8904; (c) L. Huo, Z. Li, X. Guo, Y. Wu, M. Zhang, L. Ye, S. Zhang and J. Hou, *Polym. Chem.*, 2013, **4**, 3047; (d) B.-G. Kim, X. Ma, C. Chen, Y. Ie, E. W. Coir, H. Hashemi, Y. Aso, P. F. Green, J. Kieffer and J. Kim, *Adv. Funct. Mater.*, 2013, **23**, 439.
- 5 Review on DTP-based materials: S. C. Rasmussen and S. J. Evenson, *Prog. Polym. Sci.*, 2013, **38**, 1773.
- 6 DTP-based copolymers for PSC's: (a) W. Yue, Y. Zhao, S. Shao, H. Tian, Z. Xie, Y. Geng and F. Wang, *J. Mater. Chem.*, 2009, **19**, 2199; (b) E. Zhou, Q. Wei, S. Yamakawa, Y. Zhang, K. Tajima, C. Yang and K. Hashimoto, *Macromolecules*, 2010, **43**, 821; (c) M. Shi, L. Fu, X. Hu, L. Zuo, D. Deng, J. Chen and H. Chen, *Polym. Bull.*, 2011, **68**, 1867; (d) E. Zhou, J. Cong, L. Tajima, C. Yang and K. Hashimoto, *Macromol. Chem. Phys.*, 2011, **212**, 305; (e) X. Hu, M. Shi, L. Zuo, Y. Nan, Y. Liu, L. Fu and H. Chen, *Polymer*, 2011, **52**, 2559; (f) X. Zhang, J. W. Shim, S. P. Tiwari, Q. Zhang, J. E. Norton, P.-T. Wu, S. Barlow, S. A. Jenekhe, B. Kippelen, J.-L. Brédas and S. R. Marder, *J. Mater. Chem.*, 2011, **21**, 4971; (g) E. Zhou, J. Cong, K. Tajima, C. Yang, K. Hashimoto, *J. Phys. Chem. B*, 2012, **116**, 2608; (h) B. Burkhart, P. P. Khlyabich and B. C. Thompson, *J. Photon. Energy* 2012, **2**, 021002.
- 7 J. Liu, R. Zhang, G. Sauvé, T. Kowalewski and R. D. McCullough, *J. Am. Chem. Soc.*, 2008, **130**, 13167.
- 8 (a) L. E. Polander, A. Yella, J. Teuscher, R. Humphry-Baker, B. F. E. Curchod, N. A. Astani, P. Gao, J.-E. Moser, I. Tavernelli, U. Rothlisberger, M. Grätzel, Md. K. Nazeeruddin and J. Frey, *Chem. Mater.*, 2013, **25**, 2642; (b) N. Cai, J. Zhang, M. Xu, M. Zhang and P. Wang, *Adv. Funct. Mater.*, 2013, **23**, 3539.
- 9 M. Weidelener, C. D. Wessendorf, J. Hanisch, E. Ahlswede, G. Götz, M. Lindén, G. Schulz, E. Mena-Osteritz, A. Mishra and P. Bäuerle, *Chem. Commun.*, 2013, **48**, 10865.
- 10 S. J. Evenson and S. C. Rasmussen, *Org. Lett.*, 2010, **12**, 4054.
- 11 J. Kesters, T. Ghoo, H. Penxten, J. Drijkoningen, T. Vangerven, D. M. Lyons, B. Verreet, T. Aernouts, L. Lutsen, D. Vanderzande, J. Manca and W. Maes, *Adv. Energy Mater.*, 2013, **3**, 1180.
- 12 S. J. Evenson, T. M. Pappenfus, M. C. R. Delgado, K. R. Radke-Wohlers, J. T. L. Navarrete and S. C. Rasmussen, *Phys. Chem. Chem. Phys.*, 2012, **14**, 6101.
- 13 R. Martin, C. H. Larsen, A. Cuenca and S. L. Buchwald, *Org. Lett.*, 2007, **9**, 3379.
- 14 E. Khor, S. C. Nd, H. C. Li and S. Chai, *Heterocycles*, 1991, **32**, 1805.
- 15 D. Kaufmann, M. Bialer, J. A. Shimshoni, M. Devor and B. Yagen, *J. Med. Chem.*, 2009, **52**, 7236.
- 16 G. H. Werstuck, A. J. Kim, T. Brenstrum, S. A. Ohnmacht, E. Panna and A. Capretta, *Bioorg. Med. Chem. Lett.*, 2004, **14**, 5465.
- 17 K. Pilgram, M. Zupan and R. Sikes, *J. Heterocyclic Chem.*, 1970, **7**, 629.
- 18 I. Osaka, G. Sauvé, R. Zhang, T. Kowalewski and R. D. McCullough, *Adv. Mater.*, 2007, **19**, 4160.
- 19 H. Zhou, L. Yang, A. C. Stuart, S. C. Price, S. Liu and W. You, *Angew. Chem., Int. Ed.*, 2011, **50**, 2995.
- 20 (a) S. Van Mierloo, A. Hadipour, M. Spijkman, N. Van den Brande, B. Ruttens, J. Kesters, J. D'Haen, G. Van Assche, D. M. De Leeuw, T. Aernouts, J. Manca, L. Lutsen, D. J. Vanderzande and W. Maes, *Chem. Mater.*, 2012, **24**, 587; (b) T.-Y. Chu, J. Lu, S. Beaupré, Y. Zhang, J.-R. Pouliot, J. Zhou, A. Najari, M. Leclerc and Y. Tao, *Adv. Funct. Mater.*, 2012, **22**, 2345; (c) R. S. Ashraf, B. C. Schroeder, H. A. Bronstein, Z. Huang, S. Thomas, R. J. Kline, C. J. Brabec, P. Rannou, T. D. Anthopoulos, J. R. Durrant and I. McCulloch, *Adv. Mater.*, 2013, **25**, 2029.
- 21 Y. Zhao, N. E. Schultz and D. G. Truhlar, *J. Chem. Phys.*, 2005, **123**, 161103.
- 22 J. Tomasi and M. Persico, *Chem. Rev.*, 1994, **94**, 2027; (b) J. Tomasi, B. Mennucci and R. Cammi, *Chem. Rev.*, 2005, **105**, 299.
- 23 M. J. Frisch, G. W. Trucks, H. B. Schlegel, G. E. Scuseria, M. A. Robb, J. R. Cheeseman, G. Scalmani, V. Barone, B. Mennucci, G. A. Petersson, H. Nakatsuji, M. Caricato, X. Li, H. P. Hratchian, A. F. Izmaylov, J. Bloino, G. Zheng, J. L. Sonnenberg, M. Hada, M. Ehara, K. Toyota, R. Fukuda, J. Hasegawa, M. Ishida, T. Nakajima, Y. Honda, O. Kitao, H. Nakai, T. Vreven, J. A. Montgomery Jr., J. E. Peralta Jr., F. Ogliaro, M. Bearpark, J. J. Heyd, E. Brothers, K. N. Kudin, V. N. Staroverov, R. Kobayashi, J. Normand, K. Raghavachari, A. Rendell, J. C. Burant, S. S. Iyengar, J. Tomasi, M. Cossi, N. Rega, J. M. Millam, M. Klene, J. E. Knox, J. B. Cross, V. Bakken, C. Adamo, J. Jaramillo, R. Gomperts, R. E. Stratmann, O. Yazyev, A. J. Austin, R. Cammi, C. Pomelli, J. W. Ochterski, R. L. Martin, K. Morokuma, V. G. Zakrzewski, G. A. Voth, P. Salvador, J. J. Dannenberg, S. Dapprich, A. D. Daniels, Ö. Farkas, J. B. Foresman, J. V. Ortiz, J. Cioslowski and D. J. Fox, Gaussian 09, Revision A.1, Gaussian, Inc., Wallingford CT, 2009.
- 24 (a) Y. Zou, A. Najari, P. Berrouard and S. Beaupré, *J. Am. Chem. Soc.*, 2010, **132**, 5330; (b) Y. Zhang, S. K. Hau, H.-L. Yip, Y. Sun, O. Acton and A. K.-Y. Jen, *Chem. Mater.*, 2010, **22**, 2696; (c) C. Piliago, T. W. Holcombe, J. D. Douglas, C. H. Woo, P. M. Beaujuge and J. M. Fréchet, *J. Am. Chem. Soc.*, 2010, **132**, 7595; (d) M.-C. Yuan, M.-Y. Chiu, S.-P. Liu, C.-M. Chen and K.-H. Wei, *Macromolecules*, 2010, **43**, 6936; (e) Y.-R. Hong, H.-K. Wong, L. C. H. Moh, H.-S. Tan and Z.-K. Chen, *Chem. Commun.*, 2011, **47**, 4920; (f) J. Jo, A. Pron, P. Berrouard, W. L. Leong, J. D. Yuen, J. S. Moon, M. Leclerc and A. J. Heeger, *Adv. Energy Mater.*, 2012, **2**, 1397; (g) Y.-L. Chen, C.-Y. Chang, Y.-J. Cheng and C.-S. Hsu, *Chem. Mater.*, 2012, **24**, 3964; (h) J. Yuan, Z. Zhai, H. Dong, J. Li, Z. Jiang, Y. Li and W. Ma, *Adv. Funct. Mater.*, 2013, **23**, 885; (i) S. Shi, P. Jiang, S. Yu, L. Wang, X. Wang, M. Wang, H. Wang, Y. Li and X. Li, *J. Mater. Chem. A*, 2013, **1**, 1540; (j) H. Zhong, Z. Li, F. Deledalle, E. C. Fregoso, M. Shahid, Z. Fei, C. B. Nielsen, N. Yaacobi-Gross, S.

- Rossbauer, T. D. Anthopoulos, J. R. Durrant and M. Heeney, *J. Am. Chem. Soc.*, 2013, **135**, 2040.
- 25 O. Douhéret, L. Lutsen, A. Swinnen, M. Bresselge, K. Vandewal, L. Goris and J. Manca, *Appl. Phys. Lett.*, 2006, **89**, 032107.
- 5 26 Reviews on CPE's for optoelectronic applications: (a) F. Huang, H. Wu and Y. Cao, *Chem. Soc. Rev.*, 2010, **39**, 2500; (b) A. Duarte, K.-Y. Pu, B. Liu and G. C. Bazan, *Chem. Mater.*, 2011, **23**, 501; (c) H.-L. Yip and A. K.-J. Jen, *Energy Environ. Sci.*, 2012, **5**, 5994; (d) C. Duan, K. Zhang, C. Zhong, F. Huang and Y. Cao, *Chem. Soc. Rev.*, 10 2013, **42**, 9071.
- 27 (a) J. Fang, B. H. Wallikewitz, F. Gao, G. Tu, C. Müller, G. Pace, R. H. Friend and W. T. S. Huck, *J. Am. Chem. Soc.*, 2011, **133**, 683; (b) J. H. Seo, A. Gutacker, Y. Sun, H. Wu, F. Huang, Y. Cao, U. Scherf, A. J. Heeger and G. C. Bazan, *J. Am. Chem. Soc.*, 2011, **133**, 8416;
- 15 (c) T. Yang, M. Wang, C. Duan, X. Hu, L. Huang, J. Peng, F. Huang and X. Gong, *Energy Environ. Sci.*, 2012, **5**, 8208; (d) Y. Chen, Z. Jiang, M. Gao, S. E. Watkins, P. Lu, H. Wang and X. Chen, *Appl. Phys. Lett.*, 2012, **100**, 203304; (e) C. Duan, W. Cai, B. B. Y. Hsu, C. Zhong, K. Zhang, C. Liu, Z. Hu, F. Huang, G. C. Bazan, A. J. Heeger and Y. Cao, *Energy Environ. Sci.*, 2013, **6**, 3022.
- 20 28 (a) T. Ghoos, J. Brassinne, C.-A. Fustin, J.-F. Gohy, M. Defour, N. Van den Brande, B. Van Mele, L. Lutsen, D. J. Vanderzande and W. Maes, *Polymer*, 2013, **54**, 6293; (b) T. Ghoos, O. Malinkiewicz, B. Conings, J. Manca, L. Lutsen, D. Vanderzande, H. J. Bolink and W. Maes, *RSC Adv.*, 2013, **3**, 25197.
- 25 29 During final redaction of this manuscript, Chen *et al.* reported on N-acyl-DTP-based PSC's with efficiencies up to 3.95% (employing a diamine-modified fullerene cathode interlayer material): D. Hong, M. Lv, M. Lei, Y. Chen, P. Lu, Y. Wang, J. Zhu, H. Wang, M. Gao, S. E. Watkins and X. Chen, *ACS Appl. Mater. Interfaces*, 2013, **5**, 10995.
- 30

N-acylation of dithieno[3,2-*b*:2',3'-*d*]pyrrole (DTP) leads to enhanced open-circuit voltages and hence higher power conversion efficiencies in polymer solar cells.

